Structure and Properties of Fe_4 with Different Coverage by C and CO

G. L. Gutsev* and M. D. Mochena

Department of Physics, Florida A&M University, Tallahassee, Florida 32307

C. W. Bauschlicher, Jr.

Mail Stop 230-3 NASA Ames Research Center, Moffett Field, California 94035

Received: July 28, 2004; In Final Form: October 6, 2004

The electronic and geometrical structure of neutral and singly charged Fe_4C_2, $Fe_4C(CO)$, $Fe_4(CO)_2$, Fe_4C_2-CO, $Fe_4C(CO)_2$, Fe_4C_3, and $Fe_4(CO)_3$ are studied using density functional theory with a generalized gradient approximation. It is found that the Fe_4C_2 and $Fe_4C_2(CO)$ species possess two isomers with separated and dimerized carbon atoms. The latter isomers are lower in total energy by ~0.3 eV. The Fe_4C_3 species possess three isomers corresponding to: a C_2 dimer and one separated carbon atom (the lowest energies), a C_3 trimer (intermediate energies), and three separated carbon atoms (the highest energies). The lowest energy dissociation channel corresponds to the loss of CO, except for $Fe_4(CO)_2$ and $Fe_4C(CO)_2^+$, where the loss of carbon dioxide is the lowest. The computed total energies are used to estimate the energetics of the Boudouard-like disproportionation reactions, $Fe_4C_n(CO)_m + CO \rightarrow Fe_4C_{n+1}(CO)_{m-1} + CO_2$. It is found that the most exothermic reaction in the series is $Fe_4C(CO)^+ + CO \rightarrow Fe_4C_2^+ + CO_2$ (by ~0.3 eV).

Introduction

Carbon single-walled nanotubes (SWNTs) exhibit many unique and useful physical and chemical properties[1] and have been proposed for use in various technological applications such as sensors, composite materials, hydrogen storages, and computer memories. Carbon nanotube manufacturing methods include laser vaporization of metal-doped carbon electrodes,[2] chemical vapor deposition of carbon-containing species such as C_2H_4, CH_4, C_2H_5OH, etc.,[3] on supported metal catalysts,[4] and the high-pressure CO (HiPco) process.[5] In the latter process, SWNTs grow from CO feedstock under high-pressure, high-temperature conditions. Catalyzing iron clusters are formed in situ by thermal decomposition of iron pentacarbonyl, $Fe(CO)_5$, and SWNTs are believed to nucleate and grow via the CO Boudouard disproportionation reaction: $CO + CO \rightarrow C_{SWNT} + CO_2$. The HiPco process is continuous and allows production of SWNTs in large amounts.[6] However, the growth mechanisms are not well understood. Chemical reaction models[7,8] with reaction rates derived from literature predicted a growth rate, which is ~1 order of magnitude higher than the measured one, regardless of the nucleation rate.

To obtain some insight into the formation of the iron catalyst and on the carbon nucleation, one may resort to theoretical chemistry methods. Schaefer et al.[9] tested a number of methods including Hartree−Fock (HF), density functional theory with generalized gradient approximation (DFT-GGA), and hybrid HF-DFT approaches for the homonuclear 3d-metal dimers and concluded that the results of DFT-GGA calculations are most consistent with experimental data. Using different DFT-GGA methods, we performed calibration calculations for monocarbides, MC,[10] monocarbonyls, MCO,[11] and homonuclear 3d-metal dimers[12] and found that different DFT-GGA methods produce rather similar results. Our DFT-GGA computations of clusters Fe_n, Fe_n^-, and Fe_n^+[13] as well as Fe_nO and Fe_nO[14] ($n \leq 6$) have shown good agreement with experimental data. Therefore, one could anticipate that the DFT-GGA would yield reliable results for the interactions of iron clusters with different species.

Our DFT-GGA study of neutral and singly charged clusters Fe_nC[15] and Fe_nCO[16] ($n \leq 6$), allowed us to estimate the Fe_n−C and Fe_n−CO binding energies along with the energetics of the $Fe_nCO + CO \rightarrow Fe_nC + CO_2$ Boudouard reactions. It was found that the reactions with $n = 4$ and $n = 6$ are slightly exothermic. The results of our computations are in good agreement[16] with experimental data available for FeCO and Fe_2CO, which lends support to the reliability of computations for other species.

The Fe_3^+, Fe_4^+, and Fe_5^+ clusters are known[17] to catalyze the growth of benzene from ethylene and cyclopropane in a low-pressure gas-phase process. Recent DFT-GGA studies[18,19] found that neutral Fe_4 is capable of catalyzing the benzene growth as well.

Our present work is aimed at a DFT-GGA study of the Fe_4, Fe_4^-, and Fe_4^+ clusters with different C and CO coverage. Computed total energies of the ground-state clusters are used to estimate the energetics of CO disproportionation reactions, $Fe_4C_n(CO)_m^{0/-/+} + CO \rightarrow Fe_4C_{n+1}(CO)_{m-1}^{0/-/+} + CO_2$ ($n + m \leq 3$). We report optimized geometries, harmonic vibration frequencies, and fragmentation energies of all computed species as well as adiabatic electron affinities (EA) and ionization energies (IE) of the neutral clusters.

Computational Details

The Gaussian 98 program[20] was used. We have used the 6-311+G* basis set:[21−24] (15s11p6d1f)/[10s7p4d1f] for Fe and (12s6p1d)/[5s4p1d] for C and O. Our previous study[13] of bare iron clusters showed that results obtained using many of the DFT-GGA methods included in Gaussian 98 are rather similar; however, the BPW91 vibrational frequencies appear to be less

* Corresponding author. E-mail: gennady.gutsev@famu.edu.

10.1021/jp046635s CCC: $27.50
Published on Web 11/26/2004

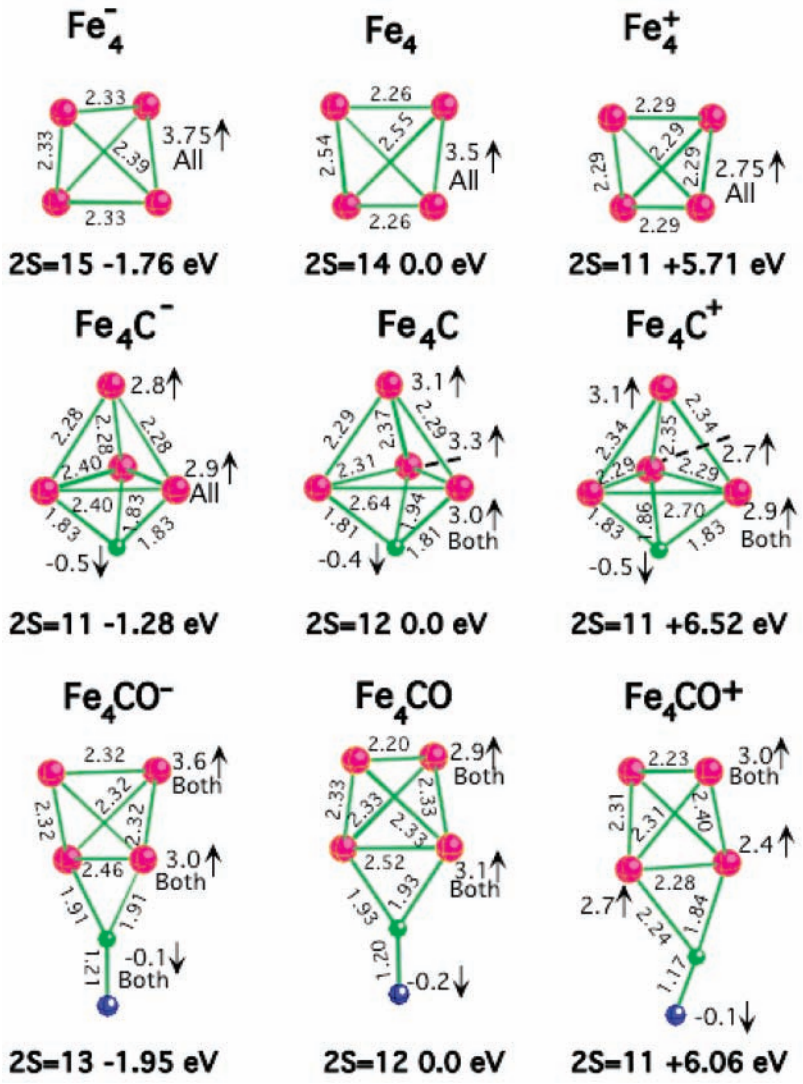

Figure 1. Geometrical structures and excess spin densities at atoms of the ground states of Fe_4, Fe_4C, Fe_4CO, and their ions. Bond lengths are in angstroms.

sensitive to the integration quality than some of the other functionals. On this ground, we choose the BPW91 method, where the exchange-correlation functional is composed of the Becke exchange[25] and the Perdew-Wang correlation.[26]

The geometry of each neutral $Fe_4C_n(CO)_m$ was optimized without imposing any symmetry constraints beginning with 12 unpaired electrons, which is the number in the ground-state clusters Fe_4C[15] and Fe_4CO,[16] while the starting number of unpaired electrons in the ions was chosen as the number of unpaired electrons in the corresponding ground-state neutrals plus one. Optimizations were performed for all lower numbers of unpaired electrons and for higher numbers until their further increase results in the states whose total energies are above dissociation asymptote. Each geometry optimization was followed by harmonic vibrational frequency calculations (computed using analytical second derivatives), to confirm that the optimized geometry corresponds to a minimum.

Our reported electron affinities and ionization energies are computed as the differences in total electronic energies corrected for the zero-point vibrational energies (ZPVEs) and correspond to adiabatic values. Fragmentation energies, computed as the differences in total energies of a species and their decay constituents, are corrected for the ZPVEs. We compute atomic spin densities using both Mulliken[27] and natural atomic orbital[28,29] approaches. Generally, the values obtained in the both approaches are nearly the same. The numbers given in the figures are obtained using Mulliken analysis.

Geometrical Structures

We classify the states by 2*S*, which is the number of majority (α or spin-up) electrons minus the number of minority (β or spin-down) electrons, or $2S = N\uparrow - N\downarrow$. The previously optimized ground states of Fe_4,[13] Fe_nC,[15] Fe_nCO,[16] and their ions are presented in Figure 1 for comparison purposes. Given in the figure are the bond lengths (in Å) and the excess spin densities, which are computed using the Mulliken population analysis. The ground-state total energies of the corresponding neutral clusters are taken as zero. Energy shifts of the anions correspond to the adiabatic electron affinities taken with the opposite sign, and the energy shifts of the cations correspond to the adiabatic ionization energies. As seen in Figure 1, the carbon atom is three-coordinate while CO is two-coordinate. Attachment of either C or CO reduces the difference in the number of spin-up and spin-down electrons with respect to those in the bare iron clusters Fe_4 and Fe_4^- while this number is the same in Fe_4^+, Fe_4C^+, and Fe_4CO^+.

The second carbon atom may attach to an Fe_3 face and decrease the 2*S* difference by 2 or dimerize with the first carbon

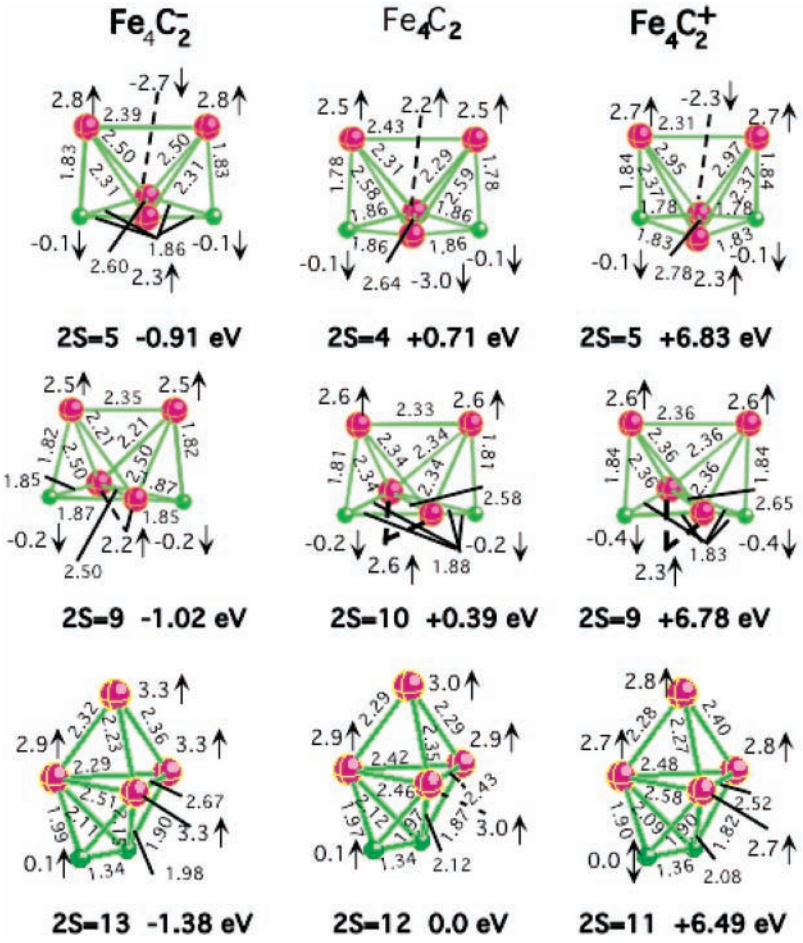

Figure 2. Geometrical structures and excess spin densities at atoms of the ground and lowest excited states of $Fe_4C_2^-$, Fe_4C_2, and $Fe_4C_2^+$.

atom without changing the number of unpaired electrons (compare Figures 1 and 2). The isomers with dimerized carbon correspond to the ground states of Fe_4C_2, $Fe_4C_2^-$, and $Fe_4C_2^+$, which are ~0.3 eV lower than the species with two separate carbon atoms. Excited states include a 3↑1↓-antiferrimagnetic branch ("3↑1↓" means that there are three spin-up and one spin-down excess spin densities at the Fe sites) initiated by a neutral $2S = 4$ state. In the bare Fe_4 cluster,[30] the 3↑1↓-antiferrimagnetic states have 4, 6, or 8 unpaired electrons, while the 2↑2↓-type possesses 0 or 2 unpaired electrons. However, the antiferrimagnetic states of Fe_4 are above the ground ferromagnetic state by at least 1 eV, while the gap decreases to 0.71 eV in Fe_4C_2 and to only 0.34 eV in $Fe_4C_2^+$. Significant elongations of Fe−Fe bond lengths with respect to those in the ground-state structures are observed in antiferrimagnetic states of Fe_4C_2 and $Fe_4C_2^+$, while no appreciable geometric change is found for $Fe_4C_2^-$.

Attachment of CO to Fe_4C, Fe_4C^-, and Fe_4C^+ does not reduce their differences in the number of spin-up and spin-down electrons as is seen in Figure 3. Carbon monoxide attaches to a single Fe atom in the ground states of $Fe_4C(CO)$ and $Fe_4C(CO)^-$, while it is two-coordinate in $Fe_4C(CO)^+$. In both ground and excited states, the separated carbon atom is bound to a face of the Fe_4 cluster.

In the ground-state $Fe_4(CO)_2$ and $Fe_4(CO)_2^+$ species, both COs are three-coordinate, while one CO is one-coordinate in the ground-state anion (see Figure 4). The lowest excited states have various geometrical shapes, and the energy separation with the ground states is rather small. This variety may be related to low binding energies of carbon monoxide. Comparing Figures 1 and 4, one finds that the $2S$ values in the ground-state $Fe_4(CO)_2$ species are the same as in the corresponding Fe_4CO species.

Like the Fe_4C_2 species, the neutral and singly charged $Fe_4C_2(CO)$ species possess two isomers in one of which two carbons are dimerized and in the other isomer the carbon atoms are separated (see Figure 5). The number of spin-up and spin-down electrons of the two isomers $Fe_4C_2(CO)$ is the same as those of the analogous isomers Fe_4C_2. This is also true for $Fe_4C_2^-$ with two separated carbons and $Fe_4C_2^+$ with a C_2 dimer. For $Fe_4C_2^-$ with a C_2 dimer, adding a CO decreases the $2S$ value by 2, while for $Fe_4C_2^+$ with separated carbon atoms, the difference decreases by 4 when CO attaches (compare Figures 2 and 5). The latter state of $Fe_4C_2(CO)^+$ is a 3↑1↓-antiferrimagnetic state that is 0.27 eV above the ground state, while a ferromagnetic state with the same $2S$ as that of ground-state $Fe_4C_2^+$ is by 0.42 eV above the ground state. As is seen from Figure 5, carbon monoxide is one-coordinate in the isomers with separated carbon atoms and is two-coordinate in the isomers with dimerized carbon.

Attachment of carbon atom to $Fe_4(CO)_2$ results in the decrease of the $2S$ value in ground-state $Fe_4C(CO)_2$ by 4 with respect to that in ground-state $Fe_4(CO)_2$. In addition, one CO group becomes one-coordinate (compare Figures 4 and 6). The $2S$ value decreases by 2 in ground-state $Fe_4C(CO)_2^-$ with respect to that in ground-state $Fe_4(CO)_2^-$, and a three-coordinate CO group becomes two-coordinate. The lowest state of $Fe_4C(CO)_2^+$ has $2S = 5$; i.e., it has the same $2S$ as the lowest state of $Fe_4C_2(CO)^+$ with separated carbons. This state is a 3↑1↓-antiferrimagnetic state and is nearly degenerate in total energy with a

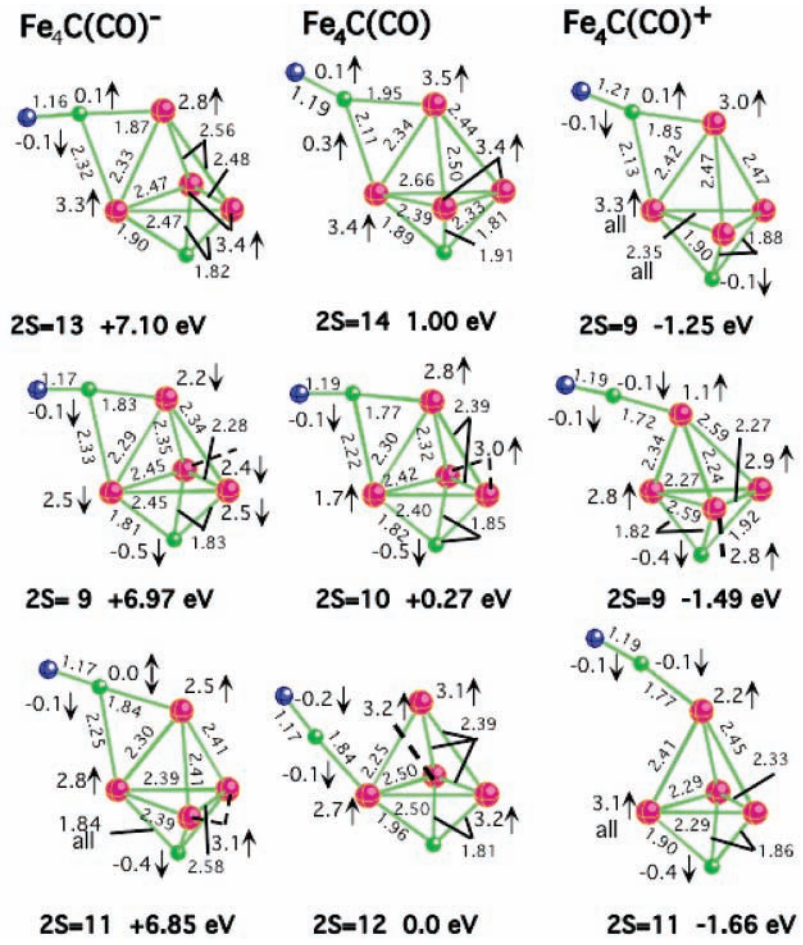

Figure 3. Structures of the ground and lowest excited states of $Fe_4C(CO)^-$, $Fe_4C(CO)$, and $Fe_4C(CO)^+$.

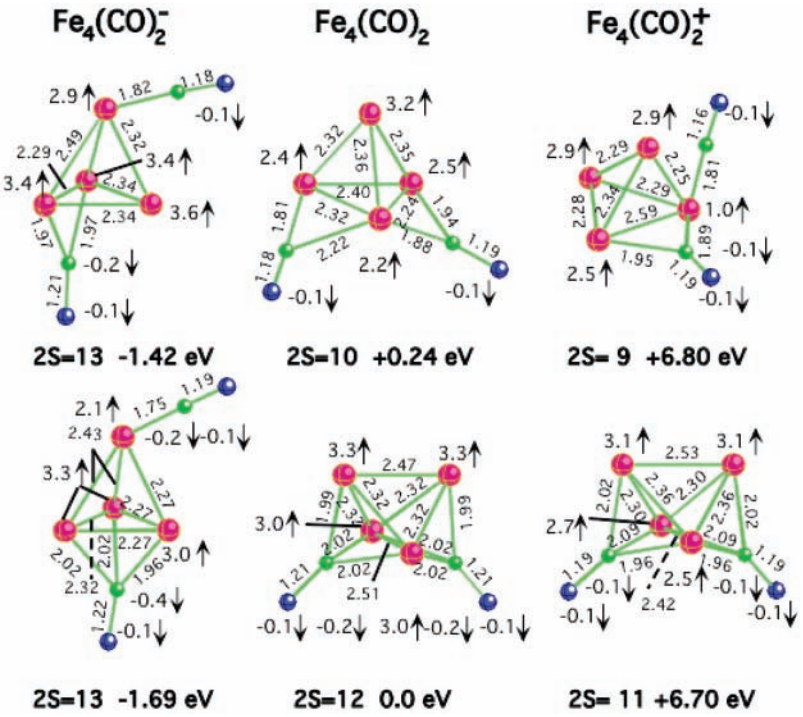

Figure 4. Structures of the ground and lowest excited states of $Fe_4(CO)_2^-$, $Fe_4(CO)_2$, and $Fe_4(CO)_2^+$.

2↑2↓-antiferromagnetic $2S = 1$ state. The lowest ferromagnetic state of the cation with $2S = 12$ is above the ground state by 0.18 eV.

The difference in the number of spin-up and spin-down electrons is reduced by 2 in ground-state $Fe_4(CO)_3$ with respect to ground-state $Fe_4(CO)_2$ (compare Figures 4 and 7). The

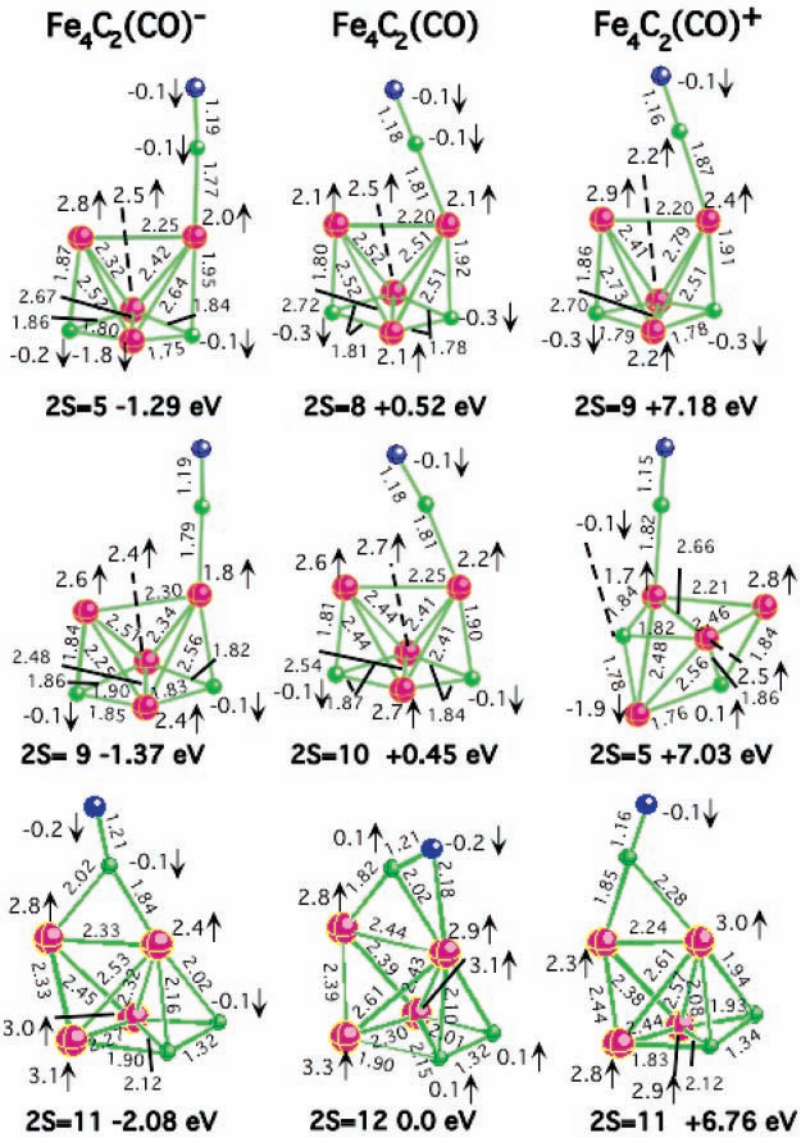

Figure 5. Structures of the ground and lowest excited states of $Fe_4C_2(CO)^-$, $Fe_4C_2(CO)$, and $Fe_4C_2(CO)^+$.

ground-state $Fe_4(CO)_3^-$ anion has the geometrical structure similar to the excited state $Fe_4(CO)_3$, and its 2*S* is also reduced by 2 with respect to ground-state $Fe_4(CO)_2^-$. A $2S = 9$ excited anion state is higher by 0.26 eV and shows all three types of CO coordination. The ground-state $Fe_4(CO)_3^+$ cation has the same 2S as ground-state $Fe_4(CO)_2^+$. All its CO groups are one-coordinate and two of them share the same Fe vertex. The lowest excited state of the cation is higher by 0.11 eV and has one three-coordinate and two two-coordinate CO groups.

Attachment of the third carbon atom to Fe_4C_2 produces three major isomers with three separated carbon atoms (the top panel in Figure 8), a C_3 trimer (the middle panel), and a C_2 dimer and one separated (the bottom panel) carbon atom. Note that the energy separation between three isomers is rather large, and two upper isomers of $Fe_4C_3^+$ have the opposite order with respect to that in Fe_4C_3 and $Fe_4C_3^-$. Ground-state Fe_4C_3 has the same 2*S* as ground-state Fe_4C_2, while the lowest isomer of Fe_4C_3 with separated carbon atoms is $3\uparrow1\downarrow$-antiferrimagnetic. For $Fe_4C_3^+$, the lowest isomer with the separate carbon atoms is $2S = 1$ and has a $2\uparrow2\downarrow$-antiferrimagnetic coupling; this state is above the cation ground state by only 0.39 eV.

Vibrational Frequencies, Electron Affinities, and Ionization Energies

Vibrational frequencies of $Fe_4C_n(CO)_{3-n}$ clusters may be divided in three groups roughly corresponding to Fe−Fe, Fe−C, and FeC−O vibrations. Vibrational frequencies of the ground-state Fe_4 cluster are[13] 104, 125, 200, 201, 228, and 347 cm^{-1}, those of the ground-state Fe_4C cluster are[16] 125, 187, 191, 223, 245, 290, 349, 521, and 693 cm^{-1}, and those of ground-state Fe_4CO are[15] 37, 65, 119, 140, 210, 245, 255, 312, 317, 360, 402, and 1753 cm^{-1}. It is seen that carbon attachments increase vibrational frequencies of the cluster, while CO attachment introduces small frequencies of the CO wagging modes as well as a large C−O frequency. The frequency of 1753 cm^{-1} of the attached CO is significantly decreased with respect to the gas-phase frequency of CO: the BPW91/6-311+G* ω_e value is 2127 cm^{-1} versus experimental[31] $\omega_e = 2158$ cm^{-1}.

As is seen from Tables 1 and 2, the presence of separated carbon atoms in $Fe_4C_m(CO)_n$ clusters manifests itself in the appearance of bands at 650−700 cm^{-1}, while dimerization of carbons in Fe_4C_2, Fe_4C_2CO, and Fe_4C_3 leads to the bands at 1421, 1483, and 1477 cm^{-1}, respectively, which are essentially lower than the gas-phase vibrational frequency of C_2 ($^1\Sigma_g^+$:

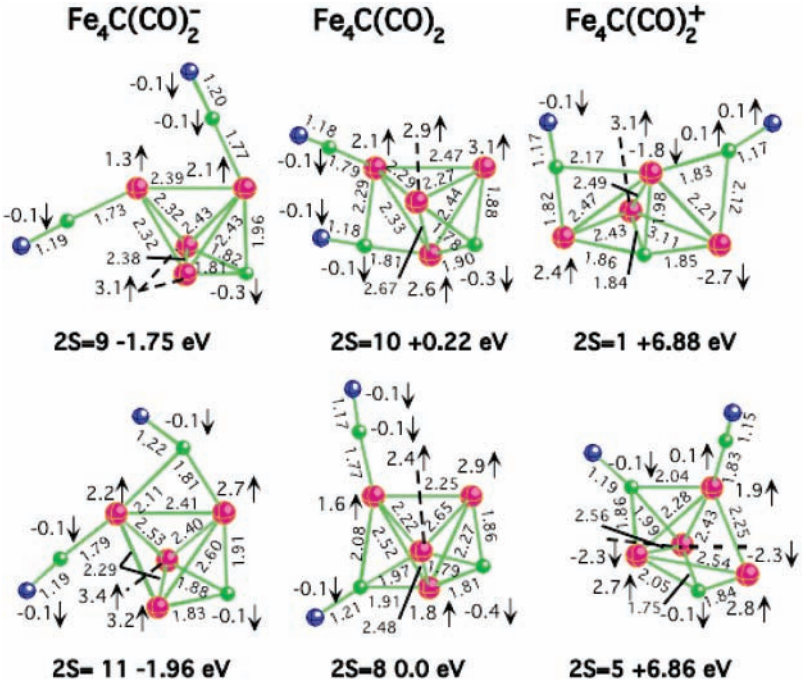

Figure 6. Structures of the ground and lowest excited states of $Fe_4C(CO)_2^-$, $Fe_4C(CO)_2$, and $Fe_4C(CO)_2^+$.

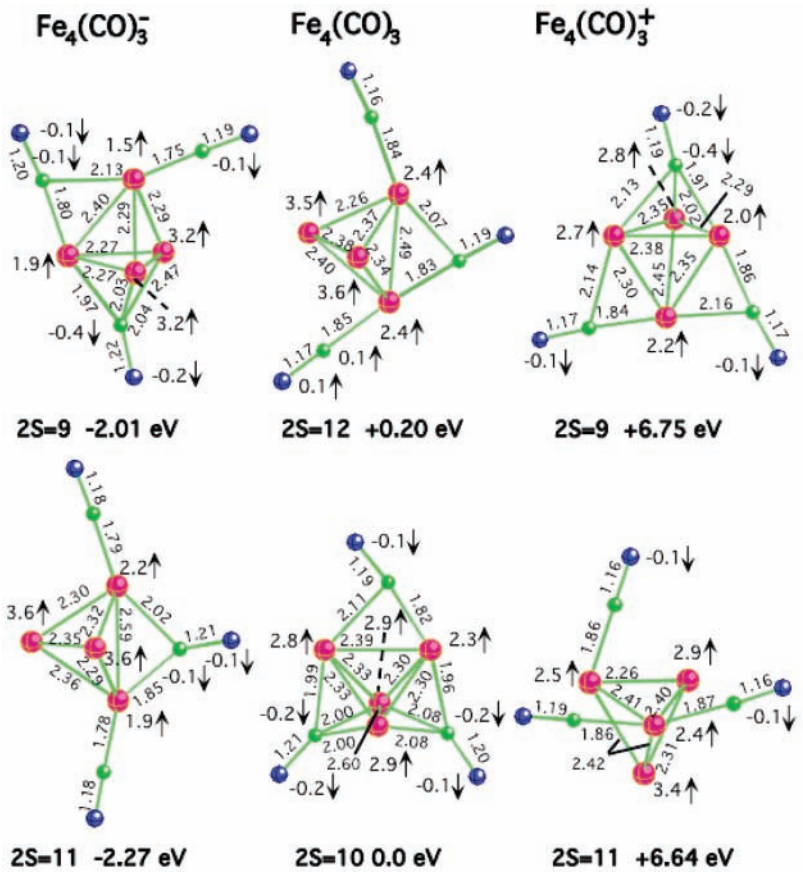

Figure 7. Structures of the ground and lowest excited states of $Fe_4(CO)_3^-$, $Fe_4(CO)_3$, and $Fe_4(CO)_3^+$.

experimental[31] and BPW91 ω_e values are 1854.7 and 1843 cm^{-1}, respectively). The C−O vibrational frequencies have a rather large splitting of 105 cm^{-1} in $Fe(CO)_3$, see Table 2.

As shown in Table 3, Fe_4C_2 possesses the smallest (1.38 eV) EA and $Fe_4(CO)_3$ the largest EA (2.22 eV). Fe_4CO has the smallest IE of 6.05 eV, while Fe_4C_3 has the largest IE of 6.98 eV. For comparison, our EA and IE of the bare Fe_4 cluster computed at the same level of theory are[13] 1.76 (experiment[32] 1.72 ± 0.08 eV) and 5.71 eV (experiment[33] 6.4 ± 0.10 eV), respectively. As seen in Table 3, there is no drastic change upon attachment of CO or C to the corresponding precursor cluster either in the EA or IE value.

Thermodynamic Stability

Fragmentation energies of the neutral and charged $Fe_4C_m(CO)_n$ clusters are presented in Table 4. The loss of CO falls in

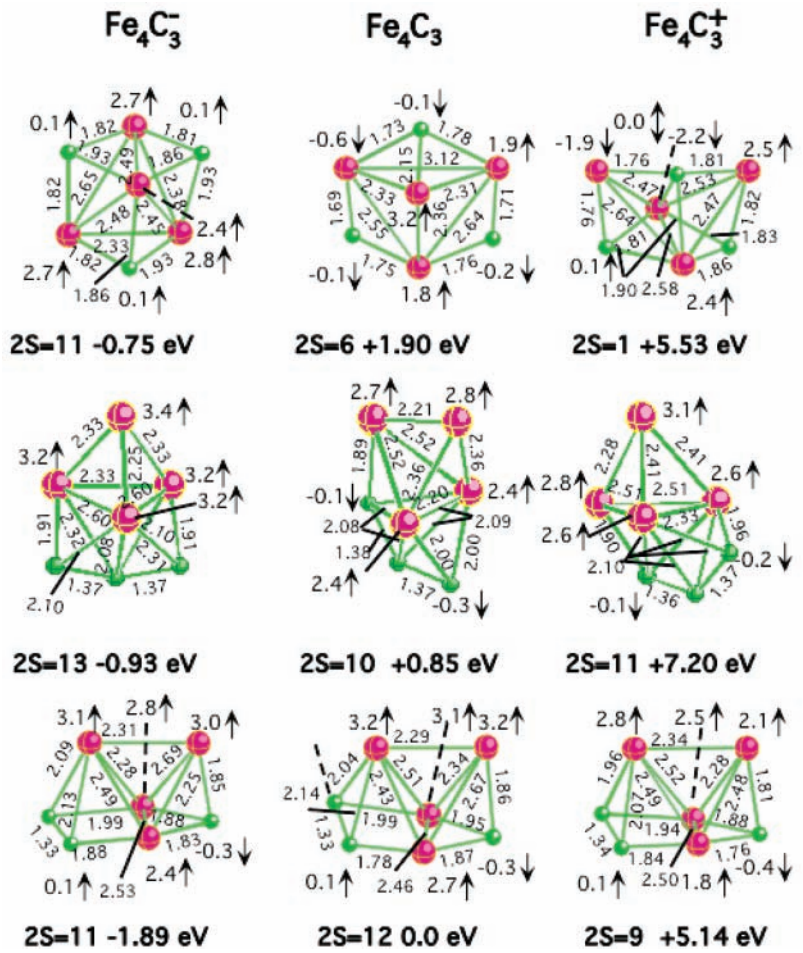

Figure 8. Structures of the ground and lowest excited states of $Fe_4C_3^-$, Fe_4C_3, and $Fe_4C_3^+$.

TABLE 1: Vibrational Frequencies of Ground-State Neutrals $Fe_4C(CO)$, $Fe_4(CO)_2$, Fe_4C_2CO, $Fe_4C(CO)_2$, and Their Ions

freq (cm^{-1})	$Fe_4C(CO)$			$Fe_4(CO)_2$			Fe_4C_2CO			$Fe_4C(CO)_2$		
	0	−	+	0	−	+	0	−	+	0	−	+
ω_1	49	30	61	110	38	75	84	65	49	49	48	38
ω_2	54	33	72	118	55	93	92	81	61	59	57	55
ω_3	79	79	120	140	101	99	127	119	75	104	78	60
ω_4	126	169	124	164	107	134	176	146	122	135	98	117
ω_5	184	187	173	190	165	135	184	150	171	157	122	121
ω_6	202	193	183	207	166	177	210	197	193	174	166	155
ω_7	226	233	196	218	223	183	234	223	209	212	182	174
ω_8	319	287	260	226	234	211	274	246	275	251	223	195
ω_9	384	333	316	227	234	217	289	300	288	261	240	239
ω_{10}	395	350	329	254	306	235	324	324	304	321	306	262
ω_{11}	431	396	408	284	316	244	334	334	327	354	366	309
ω_{12}	472	410	429	308	334	273	373	362	355	384	371	337
ω_{13}	485	507	477	315	401	315	382	413	415	396	397	376
ω_{14}	705	693	666	403	413	370	450	429	432	414	402	392
ω_{15}	1892	1810	1921	404	424	393	519	473	456	424	419	397
ω_{16}				424	538	421	548	531	596	445	493	412
ω_{17}				1686	1608	1757	1483	1504	1411	510	502	467
ω_{18}				1705	1818	1782	1658	1698	1937	561	553	579
ω_{19}										702	675	776
ω_{20}										1700	1620	1780
ω_{21}										1919	1801	2011

the intervals (1.30−1.76 eV), (1.49−2.24 eV), and (0.95−1.67 eV) for the neutral, negatively charged, and positively charged series, respectively. The next decay channel corresponds to the loss of CO_2 in species containing two and three carbon monoxides: 1.66 eV in $Fe_4(CO)_2$, 1.60 eV in $Fe_4C(CO)_2$, and 1.99 eV in $Fe_4(CO)_3$. For $Fe_4(CO)_2$, the loss of CO_2 is less endothermic than the loss of CO. The CO binding energy decreases if a cluster has attached carbon atom(s): 1.71 eV in Fe_4CO, 1.30 eV in $Fe_4C(CO)$, 1.52 eV in $Fe_4C(CO)_2$, and 1.53 eV in $Fe_4C_2(CO)$. Attachment energies of C are significantly larger than the CO binding energies: 7.06 (Fe_4C),[11] 6.61 [$Fe_4C(CO)$], 6.39 [$Fe_4C(CO)_2$], 6.45 (Fe_4C_2), and 6.60 eV in (Fe_4C_3).

Catalytic Ability of Iron Clusters

The energies of Boudouard disproportionation reactions $Fe_4C_n(CO)_m + CO \rightarrow Fe_4C_{n+1}(CO)_{m-1} + CO_2$ computed as the

TABLE 2: Vibrational Frequencies of Ground-State Fe_4C_2, Fe_4C_3, $Fe_4(CO)_3$, and Their Ions

	Fe_4C_2			Fe_4C_3			$Fe_4(CO)_3$		
freq (cm^{-1})	0	−	+	0	−	+	0	−	+
ω_1	79	96	30	122	72	71	56	39	35
ω_2	131	130	150	149	127	136	67	42	47
ω_3	187	186	202	167	189	165	105	48	52
ω_4	204	207	209	200	211	199	129	61	66
ω_5	229	235	215	235	246	217	147	79	71
ω_6	283	257	268	294	278	280	157	127	84
ω_7	315	312	314	302	297	314	173	150	147
ω_8	344	329	341	328	317	340	184	180	161
ω_9	366	353	447	354	349	378	195	203	194
ω_{10}	449	431	501	359	402	418	221	221	205
ω_{11}	561	520	617	418	426	479	228	234	230
ω_{12}	1421	1397	1314	507	482	517	264	258	285
ω_{13}				565	529	597	320	325	302
ω_{14}				694	690	726	332	355	335
ω_{15}				1477	1487	1421	337	382	338
ω_{16}							390	396	349
ω_{17}							393	427	368
ω_{18}							403	436	390
ω_{19}							411	466	410
ω_{20}							445	503	436
ω_{21}							497	527	472
ω_{22}							1675	1695	1914
ω_{23}							1712	1840	1939
ω_{24}							1780	1865	1974

TABLE 3: Adiabatic Electron Affinities and Ionization Energies of $Fe_4C_n(CO)_m$

	Fe_4CO	Fe_4C_2	$Fe_4C(CO)$	$Fe_4(CO)_2$	Fe_4C_2CO	$Fe_4C(CO)_2$	Fe_4C_3	$Fe_4(CO)_3$
EA_{ad}, eV	1.95	1.38	1.66	1.69	2.08	1.96	1.89	2.22
IE_{ad}, eV	6.05	6.49	6.84	6.68	6.76	6.84	6.98	6.63

TABLE 4: Computed Fragmentation Energies (in eV) of Neutral and Charged Fe_4CO, Fe_4C_2, $Fe_4C(CO)$, $Fe_4(CO)_2$, $Fe_4C(CO)_2$, Fe_4C_2CO, Fe_4C_3, and $Fe_4(CO)_3$

neutral		anion		cation	
channel	ΔE_{tot}	channel	ΔE_{tot}	channel	ΔE_{tot}
$Fe_4CO \rightarrow Fe_4 + CO$	1.76	$Fe_4CO^- \rightarrow Fe_4^- + CO$	1.93	$Fe_4CO^+ \rightarrow Fe_4^+ + CO$	1.41
$\rightarrow Fe_3CO + Fe$	3.04	$\rightarrow Fe_3CO^- + Fe$	3.41	$\rightarrow Fe_3CO^+ + Fe$	3.35
$Fe_4C(CO) \rightarrow Fe_4C + CO$	1.30	$Fe_4C(CO)^- \rightarrow Fe_4C^- + CO$	1.68	$Fe_4C(CO)^+ \rightarrow Fe_4C^+ + CO$	0.95
$\rightarrow Fe_4CO + C$	6.61	$\rightarrow Fe_4CO^- + C$	6.32	$\rightarrow Fe_4CO^+ + C$	5.82
$\rightarrow Fe_4C_2 + O$	6.03	$\rightarrow Fe_4C_2^- + O$	6.31	$\rightarrow Fe_4C_2^+ + O$	5.69
$\rightarrow Fe_4O + C_2$	7.03	$\rightarrow Fe_4O^- + C_2$	7.10	$\rightarrow Fe_4O^+ + C_2$	7.17
$Fe_4(CO)_2 \rightarrow Fe_4CO + CO$	1.74	$Fe_4(CO)_2^- \rightarrow Fe_4CO^- + CO$	1.49	$Fe_4(CO)_2^+ \rightarrow Fe_4CO^+ + CO$	1.13
$\rightarrow Fe_4C + CO_2$	1.66	$\rightarrow Fe_4C^- + CO_2$	2.07	$\rightarrow Fe_4C^+ + CO_2$	1.47
$\rightarrow Fe_4C_2 + O_2$	6.62	$\rightarrow Fe_4C_2^- + O_2$	6.93	$\rightarrow Fe_4C_2^+ + O_2$	6.44
$\rightarrow Fe_4O_2 + C_2$	6.96	$\rightarrow Fe_4O_2^- + C_2$	7.26	$\rightarrow Fe_4O_2^+ + C_2$	7.08
$Fe_4C(CO)_2 \rightarrow Fe_4C(CO) + CO$	1.52	$Fe_4C(CO)_2^- \rightarrow Fe_4C(CO)^- + CO$	1.82	$Fe_4C(CO)_2^+ \rightarrow Fe_4C(CO)^+ + CO$	1.52
$\rightarrow Fe_4C_2 + CO_2$	1.60	$\rightarrow Fe_4C_2^- + CO_2$	2.17	$\rightarrow Fe_4C_2^+ + CO_2$	1.26
$\rightarrow Fe_4(CO)_2 + C$	6.39	$\rightarrow Fe_4(CO)_2^- + C$	6.65	$\rightarrow Fe_4(CO)_2^+ + C$	6.23
$\rightarrow Fe_4C_3 + O_2$	6.41	$\rightarrow Fe_4C_3^- + O_2$	6.48	$\rightarrow Fe_4C_3^+ + O_2$	6.55
$Fe_4C_2CO \rightarrow Fe_4C_2 + CO$	1.53	$Fe_4C_2CO^- \rightarrow Fe_4C_2^- + CO$	2.24	$Fe_4C_2CO^+ \rightarrow Fe_4C_2^+ + CO$	1.26
$\rightarrow Fe_4C_3 + O$	6.12	$\rightarrow Fe_4C_3^- + O$	6.32	$\rightarrow Fe_4C_3^+ + O$	6.34
$\rightarrow Fe_4C(CO) + C$	6.68	$\rightarrow Fe_4C(CO)^- + C$	7.13	$\rightarrow Fe_4C(CO)^+ + C$	6.76
$\rightarrow Fe_4CO + C_2$	6.79	$\rightarrow Fe_4CO^- + C_2$	6.93	$\rightarrow Fe_4CO^+ + C_2$	6.10
$Fe_4(CO)_3 \rightarrow Fe_4(CO)_2 + CO$	1.63	$Fe_4(CO)_3^- \rightarrow Fe_4(CO)_2^- + CO$	2.16	$Fe_4(CO)_3^+ \rightarrow Fe_4(CO)_2^+ + CO$	1.67
$\rightarrow Fe_4C(CO) + CO_2$	1.99	$\rightarrow Fe_4C(CO)^- + CO_2$	2.55	$\rightarrow Fe_4C(CO)^+ + CO_2$	2.19
$\rightarrow Fe_4C_2(CO) + O_2$	6.72	$\rightarrow Fe_4C_2(CO)^- + O_2$	6.85	$\rightarrow Fe_4C_2(CO)^+ + O_2$	6.83
$Fe_4C_2 \rightarrow Fe_4C + C$	6.45	$Fe_4C_2^- \rightarrow Fe_4C^- + C$	6.61	$Fe_4C_2^+ \rightarrow Fe_4C^+ + C$	6.44
$\rightarrow Fe_4 + C_2$	7.02	$\rightarrow Fe_4^- + C_2$	6.63	$\rightarrow Fe_4^+ + C_2$	6.25
$Fe_4C_3 \rightarrow Fe_4 + C_3$	5.95	$Fe_4C_3^- \rightarrow Fe_4^- + C_3$	6.06	$Fe_4C_3^+ \rightarrow Fe_4^+ + C_3$	4.70
$\rightarrow Fe_4C + C_2$	6.54	$\rightarrow Fe_4C^- + C_2$	7.16	$\rightarrow Fe_4C^+ + C_2$	6.06
$\rightarrow Fe_4C_2 + C$	6.60	$\rightarrow Fe_4C_2^- + C$	7.10	$\rightarrow Fe_4C_2^+ + C$	6.12

differences in total energies of the reactants and products corrected for the corresponding ZPEs are presented in Table 5. As is seen, carbon nucleation is endothermic for all the neutrals except Fe_4CO and the corresponding energies are nearly independent of the Fe_4 coverage. Among the ions, there are three exothermic reactions involving $Fe_4C(CO)_2^+$ (−0.01 eV), $Fe_4C(CO)_2^-$ (−0.06 eV), and $Fe_4C(CO)^+$ (−0.26 eV), and the dependence on coverage is more pronounced than in the neutrals. On the whole, the computed energies of different channels are rather small. The largest energy among all species computed is 0.74 eV, which corresponds to the $Fe_4(CO)_3^- + CO \rightarrow Fe_4C(CO)_2^- + CO_2$ channel.

One may wonder what is energetically preferable to first add all of the CO molecules and then strip the oxygens or to stepwise

TABLE 5: Energetics of the CO_2 Formation in Neutral and Ionic Channels[a]

neutral		anion		cation	
channel	ΔE_{tot}	channel	ΔE_{tot}	channel	ΔE_{tot}
$Fe_4CO + CO \rightarrow Fe_4C + CO_2$	−0.08	$Fe_4CO^- + CO \rightarrow Fe_4C^- + CO_2$	0.58	$Fe_4CO^+ + CO \rightarrow Fe_4C^+ + CO_2$	0.34
$Fe_4C(CO) + CO \rightarrow Fe_4C_2 + CO_2$	0.08	$Fe_4C(CO)^- + CO \rightarrow Fe_4C_2 + CO_2$	0.36	$Fe_4C(CO)^+ + CO \rightarrow Fe_4C_2^+ + CO_2$	−0.26
$Fe_4(CO)_2 + CO \rightarrow Fe_4C(CO) + CO_2$	0.36	$Fe_4(CO)_2^- + CO \rightarrow Fe_4C(CO)^- + CO_2$	0.39	$Fe_4(CO)_2^+ + CO \rightarrow Fe_4C(CO)^+ + CO_2$	0.52
$Fe_4C(CO)_2 + CO \rightarrow Fe_4C_2(CO) + CO_2$	0.07	$Fe_4C(CO)_2^- + CO \rightarrow Fe_4C_2(CO)^- + CO_2$	−0.06	$Fe_4C(CO)_2^+ + CO \rightarrow Fe_4C(CO)^+ + CO_2$	−0.01
$Fe_4C_2CO + CO \rightarrow Fe_4C_3 + CO_2$	0.17	$Fe_4C_2CO^- + CO \rightarrow Fe_4C_3^- + CO_2$	0.37	$Fe_4C_2CO^+ + CO \rightarrow Fe_4C_3^+ + CO_2$	0.39
$Fe_4(CO)_3 + CO \rightarrow Fe_4C(CO)_2 + CO_2$	0.47	$Fe_4(CO)_3^- + CO \rightarrow Fe_4C(CO)_2^- + CO_2$	0.74	$Fe_4(CO)_3^+ + CO \rightarrow Fe_4C(CO)_2^+ + CO_2$	0.67

[a] All values are in eV.

add one CO and next strip the oxygen atom before adding another CO molecule. Comparing the energetics of channels presented in (1)−(3), one may conclude that (3), the stepwise approach, is more favorable.

$$Fe_4(CO)_2 + CO \rightarrow Fe_4C(CO) + CO_2 \qquad 0.36\ eV \quad (I)$$

$$+ CO \rightarrow Fe_4C_2 + CO_2 \qquad 0.08\ eV$$

$$Fe_4(CO)_3 + CO \rightarrow Fe_4C(CO)_2 + CO \qquad 0.47\ eV \quad (2)$$

$$+ CO \rightarrow Fe_4C_2(CO) + CO_2 \qquad 0.07\ eV$$

$$+ CO \rightarrow Fe_4C_3 + CO_2 \qquad 0.17\ eV$$

$$Fe_4(CO) + CO \rightarrow Fe_4C + CO_2 \qquad -0.08\ eV \quad (3)$$

$$Fe_4C + CO \rightarrow Fe_4C(CO) \qquad -1.30\ eV$$

$$Fe_4C(CO) + CO \rightarrow Fe_4C_2 + CO_2 \qquad 0.08\ eV$$

$$Fe_4C_2 + CO \rightarrow Fe_4C_2(CO) \qquad -1.53\ eV$$

$$Fe_4C_2(CO) + CO \rightarrow Fe_4C_3 + CO_2 \qquad 0.17\ eV$$

Conclusion

The results of our DFT-GGA computations on neutral and singly negatively and positively charged $Fe_4C_n(CO)_m$ species allow one to draw several conclusions:

(i) Geometries of ground and excited states of neutral and charged species are rather different in the $Fe_4C(CO)$, $Fe_4(CO)_2$, $Fe_4C(CO)_2$, and $Fe_4(CO)_3$ series.

(ii) Two isomers of the Fe_4C_2 series correspond to two separated carbon atoms and to a C_2 dimer, while Fe_4C_3 species has three isomers corresponding to three separated carbon atoms, to one C_2 dimer and one separated carbon atom, and to a C_3 trimer. In both series, the lowest energy states correspond to the species with a C_2 dimer.

(iii) Adding C reduces the difference in the number of spin-up and spin-down electrons ($2S$) of a species if there is no carbon dimerization, while adding CO does not lead often to any change in $2S$.

(iv) Antiferromagnetic states corresponding to small $2S$ numbers may approach closely ferromagnetic states with larger $2S$ numbers, especially in cations. For example, an antiferromagnetic state of Fe_4C_3 with $2S = 1$ is above the ground state of this cation with $2S = 9$ by 0.39 eV. This is in contrast with Fe_4, where antiferromagnetic states were found at energies exceeding 1 eV.

(v) The less endothermic channels correspond to the loss of carbon monoxide except for $Fe_4(CO)_2$ and $Fe_4C(CO)_2^+$, where loss of CO_2 is the least endothermic dissociation path.

(vi) Energies of Boudouard CO disproportionation reactions $Fe_4C_n(CO)_m^{0/-/+} + CO \rightarrow Fe_4C_{n+1}(CO)_{m-1}^{0/-/+} + CO_2$ ($n + m \leq 3$), are relatively small ranging from −0.26 eV ($Fe_4C(CO)^+$) to +0.74 eV ($Fe_4(CO)_3^-$).

Acknowledgment. This work was partly supported by NASA Ames Research Center through Contract NAS2-99092 to Eloret Corp. to G.L.G. This work was also supported in part by the Army High Performance Computing Research Center (AHPCRC) under the auspices of the Department of the Army, Army Research Laboratory (ARL) under Cooperative Agreement DAAD19-01-2-0014. The content of which does not necessarily reflect the position or the policy of the government, and no official endorsement should be inferred. We thank Dr. Norbert Müller for providing us with the new version of Ball&Stick software[34] used for plotting individual geometrical structures presented in the figures.

References and Notes

(1) Yakobson, B. I.; Smalley, R. E. *Am. Sci.* **1997**, *85*, 324.
(2) Journet, C.; Maser, W. K.; Bernier, P.; Loiseau, A.; Delachapelle, M. L.; Lefrant, S.; Deniard, P.; Lee, R.; Fischer, J. E. *Nature* **1997**, *388*, 756.
(3) Su, M.; Liu, J. *Chem. Phys. Lett.* **2000**, *322*, 321.
(4) Kong, J.; Cassel, A. M.; Dai, H. *Chem. Phys. Lett.* **1998**, *292*, 567.
(5) Nikolaev, P.; Bronikowski, M. J.; Bradley, R. K.; Rohmund, F.; Colbert, D. T.; Smith, K. A.; Smalley, R. E. *Chem. Phys. Lett.* **1999**, *313*, 91.
(6) Bronikowski, M. J.; Willis, P. A.; Colbert, D. T.; Smith, K. A.; Smalley, R. E. *J. Vac. Sci Technol., A* **2001**, *19*, 1800.
(7) Scott, C. D.; Povitsky, A.; Dateo, C.; Gökçen, T.; Willis, P. A.; Smalley, R. E. *J. Nanosci. Nanotechnol.* **2003**, *3*, 63; Dateo, C.; Gökçen, T.; Meyyappan, M. *J. Nanosci. Nanotechnol.* **2002**, *2*, 523, 535.
(8) Scott, C. D.; Smalley, R. E. *J. Nanosci. Nanotechnol.* **2003**, *3*, 75.
(9) Barden, C. J.; Rienstra-Kiracofe, J. C.; Schaefer, H. F., III. *J. Chem. Phys.* **2000**, *113*, 690.
(10) Gutsev, G. L.; Bauschlicher, C. W., Jr.; Andrews, L. *Theor. Chem. Acc.* **2003**, *109*, 298.
(11) Gutsev, G. L.; Bauschlicher, C. W., Jr.; Andrews, L. *Chem. Phys.* **2003**, *290*, 47.
(12) Gutsev, G. L.; Bauschlicher, C. W., Jr. *J. Phys. Chem. A* **2003**, *107*, 4755.
(13) Gutsev, G. L.; Bauschlicher, C. W., Jr. *J. Phys. Chem. A* **2003**, *107*, 7013.
(14) Gutsev, G. L.; Bauschlicher, C. W., Jr.; Zhai, H.-J.; Wang, L. S. *J. Chem. Phys.* **2003**, *119*, 11135.
(15) Gutsev, G. L.; Bauschlicher, C. W., Jr. *J. Chem. Phys.* **2003**, *119*, 3681.
(16) Gutsev, G. L.; Bauschlicher, C. W., Jr. *Chem. Phys.* **2003**, *291*, 27.
(17) Schnabel, P.; Irion, M. P.; Weil, K. G. *J. Phys. Chem.* **1991**, *95*. 9688.
(18) Chrétien, S.; Salahub, D. R. *J. Chem. Phys.* **2003**, *119*, 12279.
(19) Chrétien, S.; Salahub, D. R. *J. Chem. Phys.* **2003**, *119*, 12291.
(20) *Gaussian 98*, Revision A.11; Frisch, M. J.; Trucks, G. W.; Schlegel, H. B.; Scuseria, G. E.; Robb, M. A.; Cheeseman, J. R.; Zakrzewski, V. G.; Montgomery, J. A., Jr.; Stratmann, R. E.; Burant, J. C.; Dapprich, S.; Millam, J. M.; Daniels, A. D.; Kudin, K. N.; Strain, M. C.; Farkas, O.; Tomasi, J.; Barone, V.; Cossi, M.; Cammi, R.; Mennucci, B.; Pomelli, C.; Adamo, C.; Clifford, S.; Ochterski, J.; Petersson, G. A.; Ayala, P. Y.; Cui, Q.; Morokuma, K.; Malick, D. K.; Rabuck, A. D.; Raghavachari, K.; Foresman, J. B.; Cioslowski, J.; Ortiz, J. V.; Baboul, A. G.; Stefanov, B. B.; Liu, G.;

Liashenko, A.; Piskorz, P.; Komaromi, I.; Gomperts, R.; Martin, R. L.; Fox, D. J.; Keith, T.; Al-Laham, M. A.; Peng, C. Y.; Nanayakkara, A.; Gonzalez, C.; Challacombe, M.; Gill, P. M. W.; Johnson, B.; Chen, W.; Wong, M. W.; Andres, J. L.; Gonzalez, C.; Head-Gordon, M.; Replogle, E. S. and Pople, J. A. Gaussian, Inc., Pittsburgh, PA, 1998.

(21) Wachters, A. J. H. *J. Chem. Phys.* **1970**, *52*, 1033.

(22) Hay, P. J. *J. Chem. Phys.* **1977**, *66*, 4377.

(23) Frisch, M. J.; Pople, J. A.; Binkley, J. S. *J. Chem. Phys.* **1984**, *80*, 3265 and references therein.

(24) Raghavachari, K.; Trucks, G. W. *J. Chem. Phys.* **1989**, *91*, 1062.

(25) Becke, A. D. *Phys. Rev. A* **1988**, *38*, 3098.

(26) Perdew, J. P.; Wang, Y. *Phys. Rev. B* **1992**, *45*, 13244.

(27) Mulliken, R. S. *J. Chem. Phys.* **1955**, *23*, 1833, 1841, 2338, 2343.

(28) Reed, A. E.; Weinstock, R. B.; Weinhold, F. *J. Chem. Phys.* **1985**, *83*, 735.

(29) Reed, A. E.; Curtiss, L. A.; Weinhold, F. *Chem. Rev.* **1988**, *88*, 899.

(30) Gutsev, G. L. *Phys. Rev. B* **2002**, *65*, 132417.

(31) Huber K. P.; Herzberg, G. *Constants of Diatomic Molecules*; Van Nostrand-Reinhold: New York, 1979.

(32) Wang. L. S.; Li, X.; Zhang, H. F. *Chem. Phys*. **2000**, *262*, 53.

(33) Rohlfing, E. A.; Cox, D. M.; Kaldor, A.; Johnson, K. H. *J. Chem. Phys*. **1984**, *81*, 3846.

(34) Norbert Müller, Ball & Stick 4.0 (prerelease), molecular graphics software for MacOS X, Johannes Kepler University Linz, 2004. <http://www.orc.uni-linz.ac.at/mueller/ball_ and _stick>.